Reflection-Based Relative Localization for Cooperative UAV Teams Using Active Markers

Tim Lakemann[1], Daniel Bonilla Licea[1,2], Viktor Walter[1] and Martin Saska[1]

***Abstract*— Reflections of active markers in the environment are a common source of ambiguity in onboard visual relative localization. This work presents a novel approach for onboard relative localization in multi-robot teams that exploits these typically unwanted reflections of active markers in the environment. It operates without prior knowledge of robot size or predefined marker configurations and remains independent of surface properties, an essential feature for heterogeneous micro-aerial swarms cooperating in unknown environments. The proposed method explicitly accounts for uncertainties caused by non-flat surfaces, which are especially relevant for marine deployments. We validated the approach in both indoor and outdoor experiments, demonstrating that the proposed reflection-based localization system operates reliably without prior knowledge of team member size and achieves greater effective range (above *30 m*) and accuracy than state-of-the-art methods. The video is available at: https://youtu.be/y0zp8cIwkig.**

I. Introduction

Reliable relative localization among team members is crucial for multi-robot systems to collaboratively execute tasks safely and reliably [1]. In marine outdoor environments, Global Navigation Satellite System (GNSS) often lacks the reliability needed for close-formation flight due to degraded accuracy [2], [3]. Real-Time Kinematic (RTK) antennas enhance reliability but limit the operational space of Uncrewed Aerial Vehicles (UAVs) [3].

Onboard relative localization eliminates the dependence on external infrastructure, expands operational flexibility, and allows deployment without communication between team members. Vision-based methods provide a compact and lightweight solution [4], [5], [6]. Active markers attached to the UAVs overcome the lighting limitations of passive marker-based approaches [7], [8]. However, most such systems require prior knowledge of the marker configuration to estimate relative distance from pixel spacing [6], [8], [9].

This work addresses these limitations by introducing a novel relative localization system for multi-robot teams that uses surface reflections – typically considered undesirable and a source of ambiguity in localization systems. The method is motivated by mission scenarios with reflective surfaces such as maritime monitoring, nighttime surveillance, subterranean navigation, and warehouse operations (Fig. 1). Unlike prior works that suppress reflections via polarization filters [10], [11] or RF-based methods [12], [13], our approach actively uses them for localization without knowledge of UAV size or surface properties. By accounting for the reflection spread caused by surface irregularities and sensor uncertainties, the method improves reliability and extends the effective localization range.

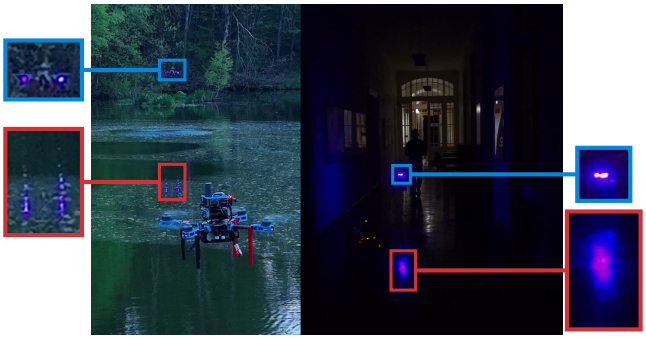

Fig. 1: Outdoor (left) and indoor dark (right) experiments: A UAV estimates the relative position by using surface reflections from active markers attached to a team member UAV. Blue boxes: the UAV with active markers. Red box: Surface reflections of emitted light.

II. Reflection-Based Localization Method

The proposed method works effectively both indoors and outdoors, regardless of UAV size or surface properties. Each UAV emits a unique blinking sequence via its Light-emitting diodes (LEDs) [14], tracked and identified using [15]. At higher exposure settings, which are required for reliable reflection detection, a single LED may segment into multiple detected regions. Nearby detections are therefore grouped via clustering, with the dominant cluster treated as the direct LED source. Clusters located vertically below are marked as reflection centroids, identified either by their blinking sequence or by geometric constraints.

While wall reflections are theoretically feasible, our experiments indicate that walls in urban indoor environments produce predominantly diffuse reflections, resulting in insufficient light intensity reaching the receiver. We therefore focus exclusively on ground and water reflections, for which a single dominant reflection can be reliably obtained.

For a calibrated fisheye camera, pixel centroids p_d (direct) and p_r (reflection) are converted into 3D unit bearing vectors via *cam2world* [16], and then corrected for the roll (ψ) and pitch (ϕ) of the observer:

$$\vec{\hat{b}}_d = \boldsymbol{R}(-\psi)\boldsymbol{R}(-\phi)\, \mathit{cam2world}(p_d), \tag{1}$$

$$\vec{\hat{b}}_r = \boldsymbol{R}(-\psi)\boldsymbol{R}(-\phi)\, \mathit{cam2world}(p_r). \tag{2}$$

The reflection center $\vec{r}$ is then computed using the observer height z_o:

$$\vec{r} = \begin{bmatrix} |z_o|\frac{\hat{x}_r}{|\hat{z}_r|} & |z_o|\frac{\hat{y}_r}{|\hat{z}_r|} & -z_o \end{bmatrix}^\top. \tag{3}$$

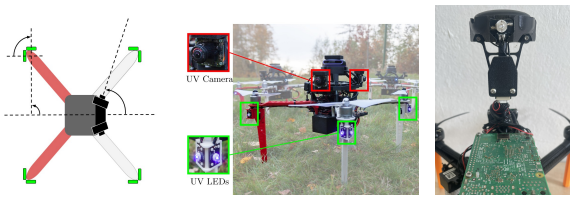

(a) (b)

Fig. 2: (a) *UVDAR* estimating position using known UV-LED spacing [14]. (b) UV-LED array on a Micro Aerial Vehicle (MAV) used in indoor experiments.

Since reflected light appears elongated due to shallow incidence angles and surface scattering, we model the reflection uncertainty as an ellipse centered at p_r, with axes defined by the farthest pixels p_v and p_h exceeding an intensity threshold σ. Applying (3) to these pixels yields $\vec{r}_v$ and $\vec{r}_h$, from which we construct a finite elliptical cone (Fig. 3) parameterized by:

$$\begin{aligned}\vec{c}_r(\gamma_r, l_r, \alpha_r, \upsilon_r) = \vec{a} + l_r\hat{\vec{d}}_r + l_r\vec{n}_1 \tan\alpha_r \cos\gamma_r \\ + l_r\vec{n}_2 \tan\upsilon_r \sin\gamma_r,\end{aligned} \tag{4}$$

where:

$$\vec{a} = [0\ 0\ -2z_0]^\top, \quad \gamma_r \in [0, 2\pi], \quad \alpha_r \in [0, \alpha_r^{\max}],$$
$$\upsilon_r \in [0, \upsilon_r^{\max}], \quad l_r \in [0, ||\vec{p}_r - \vec{a}||], \quad \hat{\vec{d}}_r = \frac{\vec{p}_r - \vec{a}}{||\vec{p}_r - \vec{a}||},$$

and $\vec{n}_1$ is a unit vector perpendicular to $\hat{\vec{d}}_r$, while $\vec{n}_2$ is a unit vector perpendicular to both $\hat{\vec{d}}_r$ and $\vec{n}_1$. A second elliptical cone is constructed around $\hat{\vec{b}}_d$ to account for camera resolution and binarization uncertainties (Fig. 3).

The intersection of the two cones defines the set of feasible transmitter locations. We estimate this via random sampling: points are drawn uniformly from within the reflection cone (4) and tested if they lie in the direct cone. Inliers are stored in the observation set $\mathcal{X}_d$, which is used for a particle filter update using a constant-velocity model with Cauchy-kernel weight updates.

III. Experiments

We evaluated the approach in indoor and marine outdoor environments against the state-of-the-art UltraViolet Direction And Ranging (*UVDAR*) method [17]. During outdoor experiments, two UAVs were used, equipped with *F450* and *Holybro X500* frames and *Intel NUC 10 i7FNK* onboard computers. In the indoor experiments an additional MAV was used with a *Raspberry Pi 5*, to underline the deployability of our method running on small-scale platforms as well as the capability of our method to work in multi-UAV scenarios. All platforms carried a fisheye camera with Ultraviolet (UV)-bandpass filter. Ground truth was provided by Ultra-wideband (UWB) (indoor) and RTK (outdoor).

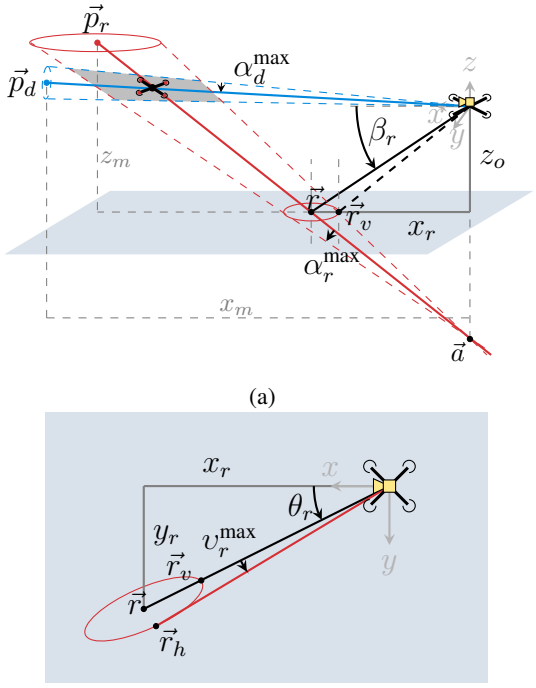

Fig. 3: (a) Side view: potential transmitter location (gray) from the intersection of two elliptical cones. (b) Top-down view: ellipse fitted to the diffuse reflection.

A. Indoor Experiments

The indoor experiments were conducted in an office hallway (Polyvinyl chloride (PVC) floor) and a corridor (tiled surface) under both daylight and nighttime conditions (Fig. 1). A single circular UV-LED array per UAV was used, highlighting platform independence. *UVDAR* requires spatially separated markers (e.g., on the arms of the UAV) and could therefore not be evaluated here. Fig. 6 shows the estimated relative position, decomposed into horizontal (Euclidean distance over x and y) and vertical (z) components, from one UAV to another UAV and to one MAV. The method achieves an Mean Absolute Error (MAE) of 1.50 ± 1.44 m in d_{xy} and 0.49 ± 0.36 m in z for the UAV, and 1.25 ± 0.93 m in d_{xy} and 0.36 ± 0.37 m in z for the MAV. The system reliably estimated the relative position of the UAV and MAV throughout the experiment. From timestamp 105 s to 155 s, the MAV was deliberately positioned in front of the UAV to cause signal interference and ambiguous reflections, therefore the system could not uniquely extract the signal from

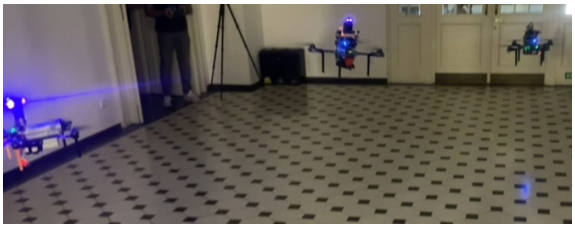

Fig. 4: Heterogeneous multi-UAV experiment

Fig. 5: Outdoor experiment: (Left) Image showing the observing UAV (white), the UAV with the active marker system (blue), and its reflections on the surface (red). (Right) Image captured onboard the UAV using a UV-bandpass filter. The centroid of the UAV equipped with active marker system (blue) and ellipse (red) of the reflection on the water surface.

the reflections. This caused the relative position estimation to fail for the occluded UAV, as full estimation requires the vector (p_d) towards the transmitting platform, which is recoverable only under Line of Sight (LoS) conditions. Note that relative bearing remains obtainable in non-LoS scenarios, but is insufficient alone for position reconstruction. The overall runtime of the method on the *Intel NUC* was approximately 82 ms, compared to 106 ms on the *Raspberry Pi 5*, underlining the capability of our method to run in real-time on resource-constrained platforms.

B. Marine Outdoor Experiments

Multiple outdoor experiments with varying exposure time settings were conducted. We observed that with a maximum exposure time of 3 ms, the camera maintained a stable frame rate (essential for reliable *UVDAR* operation) while reflections remained clearly visible at distances exceeding 20 m on the water surface.

Fig. 7 shows the three most relevant outdoor flights, comparing the relative positions obtained from our method, *UVDAR*, and the ground truth. Our reflection-based approach maintained high accuracy at distances beyond 30 m, whereas *UVDAR* struggled to provide reliable estimates past 20 m. This highlights the advantage of our approach, which operates without prior knowledge of the UAV size or the configuration of its light sources.

Tab. I summarizes the MAEs and standard deviations for each axis across all experiments, along with the *Wilcoxon p-values* and 95 % Confidence Interval (CI) of the paired differences. Along the z-axis, *UVDAR* achieved slightly lower MAE values (by 1–25 %). However, the differences were not statistically significant (p-*value* ≥ 0.05). Along the y-axis, our method reduced the MAE by 13.9 % and 58.7 % in experiments 1 and 3 (p-*value* < 0.05, 95 % CI fully below zero), whereas no statistically significant difference was observed in experiment 2. Along the x-axis (optical axis), our method reduced the MAE by 18.5–37.3 % compared to *UVDAR*, with the difference being statistically significant (p-*value* < 0.05, 95 % CI fully below zero).

Overall, our method yielded higher precision in position estimates than *UVDAR*, particularly along the x- and y-axes and at distances exceeding 30 m.

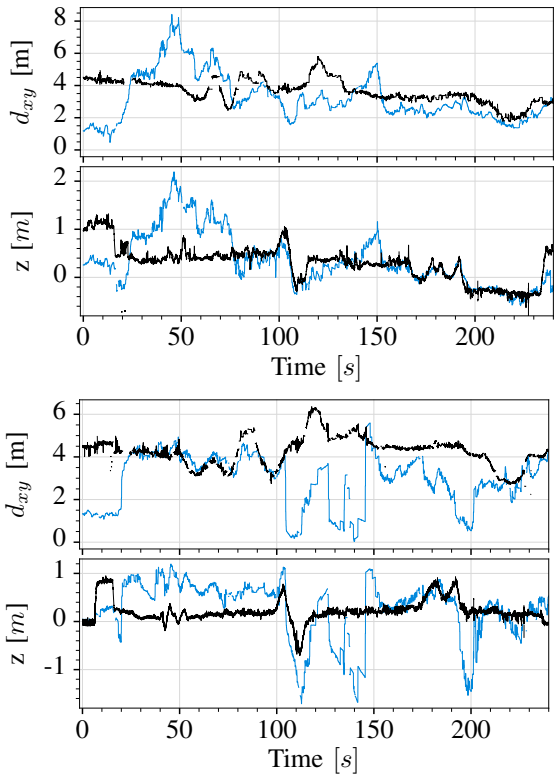

Fig. 6: Relative position estimates obtained using our approach (blue) and the ground truth from UWB (black) for the UAV (top) and MAV (bottom) during the multi-UAV experiment.

IV. Conclusion

This work presents a novel approach for onboard relative localization between tightly cooperating multi-robot teams. Our method estimates the relative position between UAVs by exploiting typically unwanted reflections of active localization markers attached to team members. By accounting for uncertainties introduced by camera resolution and surface irregularities, the proposed method operates without prior knowledge of team member sizes or surface properties. This makes it particularly well-suited for fast deployment on micro-UAVs flying in close formation in urban indoor, and marine outdoor environments. We validated our approach in indoor experiments, demonstrating reliable performance without prior knowledge of team member sizes or surface properties, and robustness to varying lighting conditions. Outdoor experiments further showed that our method outperforms current state-of-the-art approaches, particularly at greater distances (> 30 m), reducing the MAE by up to 37.3 % along the optical axis. These results demonstrate that our novel reflection-based approach provides a reliable and accurate solution for relative localization in challenging marine real-world environments.

		X			Y			Z		
		MAE[m]	p-value	95 % CI	MAE[m]	p-value	95 % CI	MAE[m]	p-value	95 % CI
1. Outdoor	Ours	3.50 ± 1.86	1.9×10^{-8}	$[-2.62, -1.61]$	1.18 ± 0.80	0.015	$[-0.26, -0.07]$	1.04 ± 1.57	0.917	$[0.15, 0.42]$
	UVDAR	5.58 ± 5.77			1.37 ± 1.09			0.78 ± 0.83		
2. Outdoor	Ours	2.42 ± 1.50	2.0×10^{-5}	$[-0.75, -0.29]$	1.73 ± 0.95	0.071	$[-0.16, 0.02]$	0.70 ± 0.47	0.009	$[-0.01, 0.07]$
	UVDAR	2.97 ± 2.14			1.76 ± 0.97			0.67 ± 0.44		
3. Outdoor	Ours	5.01 ± 4.15	2.2×10^{-11}	$[-1.95, -1.18]$	3.29 ± 1.58	0.000	$[-4.89, -4.19]$	0.98 ± 0.85	0.793	$[-0.04, 0.11]$
	UVDAR	7.00 ± 6.03			7.96 ± 5.60			0.97 ± 0.67		

TABLE I: Mean Absolute Error (MAE) and one standard deviation along the x-, y-, and z-axes, together with the *Wilcoxon p-values* and 95 % Confidence Interval (CI) of the paired differences, comparing our method with *UVDAR* in outdoor experiments.

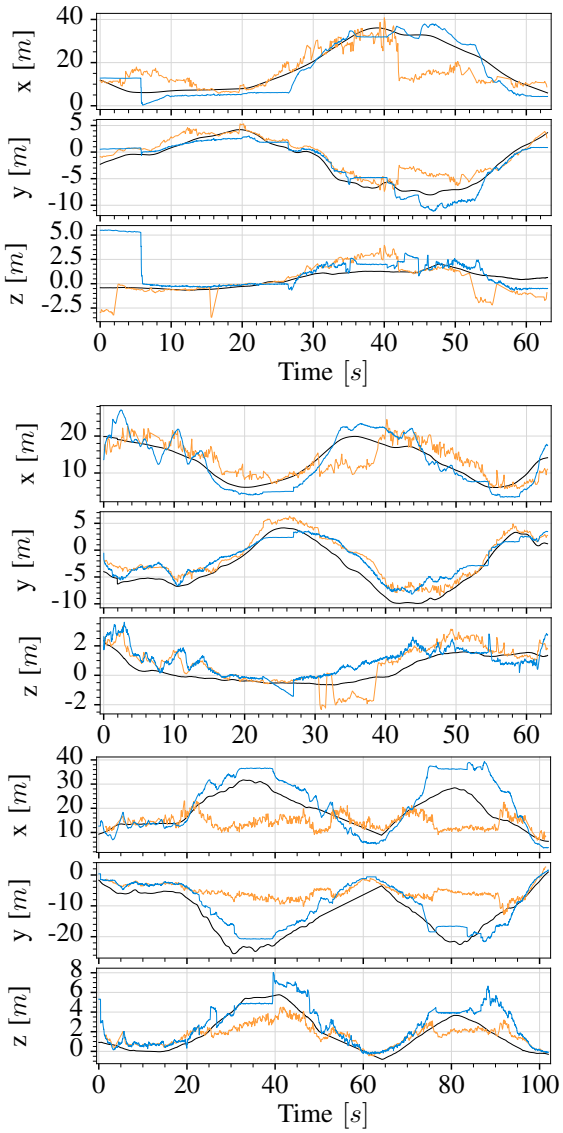

Fig. 7: Relative position estimates obtained using our approach (blue), *UVDAR* (orange), and the ground truth from RTK (black) for outdoor experiments 1–3 (from top to bottom).

REFERENCES

[1] T. H. Nguyen and L. Xie, "Relative transformation estimation based on fusion of odometry and uwb ranging data," *IEEE Transactions on Robotics*, vol. 39, no. 4, pp. 2861–2877, 2023.

[2] Z. Zhang, H. Yuan, X. He, B. Li, and J. Geng, "Best Integer Equivariant Estimation With Quality Control in GNSS RTK for Canyon Environments," *IEEE Transactions on Aerospace and Electronic Systems*, vol. 59, no. 4, pp. 4105–4117, 2023-08.

[3] T.-M. Nguyen, Z. Qiu, T. H. Nguyen, M. Cao, and L. Xie, "Distance-Based Cooperative Relative Localization for Leader-Following Control of MAVs," *IEEE Robotics and Automation Letters*, vol. 4, no. 4, pp. 3641–3648, 2019-10.

[4] H. Xu, L. Wang, Y. Zhang, K. Qiu, and S. Shen, "Decentralized Visual-Inertial-UWB Fusion for Relative State Estimation of Aerial Swarm," in *2020 IEEE International Conference on Robotics and Automation (ICRA)*, 2020-05, pp. 8776–8782.

[5] F. Schilling, F. Schiano, and D. Floreano, "Vision-Based Drone Flocking in Outdoor Environments," *IEEE Robotics and Automation Letters*, vol. 6, no. 2, pp. 2954–2961, 2021-04.

[6] L. Teixeira, F. Maffra, M. Moos, and M. Chli, "VI-RPE: Visual-Inertial Relative Pose Estimation for Aerial Vehicles," *IEEE Robotics and Automation Letters*, vol. 3, no. 4, pp. 2770–2777, 2018-10.

[7] H. Stuckey, L. Escamilla, L. R. Garcia Carrillo, and W. Tang, "Real-Time Optical Localization and Tracking of UAV Using Ellipse Detection," *IEEE Embedded Systems Letters*, vol. 16, no. 1, pp. 1–4, 2024-03.

[8] V. Walter, N. Staub, A. Franchi, and M. Saska, "UVDAR System for Visual Relative Localization With Application to Leader–Follower Formations of Multirotor UAVs," *IEEE Robotics and Automation Letters*, vol. 4, no. 3, pp. 2637–2644, 2019-07.

[9] M. Faessler, E. Mueggler, K. Schwabe, and D. Scaramuzza, "A monocular pose estimation system based on infrared leds," in *2014 IEEE International Conference on Robotics and Automation (ICRA)*, 2014, pp. 907–913.

[10] K. Berger, R. Voorhies, and L. H. Matthies, "Depth from stereo polarization in specular scenes for urban robotics," in *2017 IEEE International Conference on Robotics and Automation (ICRA)*, May 2017, pp. 1966–1973.

[11] Y. Li, S. Lin, H. Lu, S. B. Kang, and H.-Y. Shum, "Multibaseline stereo in the presence of specular reflections," in *2002 International Conference on Pattern Recognition*, vol. 3, 2002, pp. 573–576.

[12] Z. Li, P. Wang, K. Liu, and Z. Tian, "MimoLoc: Indoor Localization With Assistance of Microwave Reflection of Downlink Signal in Sub-6G MIMO Networks," *IEEE Transactions on Microwave Theory and Techniques*, vol. 72, no. 4, pp. 2655–2668, Apr. 2024.

[13] Z. Li, P. Wang, Z. Tian, and K. Liu, "TriLoc: Toward Accurate Indoor Localization With Assistance of Microwave Reflections," *IEEE Transactions on Microwave Theory and Techniques*, vol. 71, no. 6, pp. 2734–2747, Jun. 2023.

[14] D. Bonilla Licea, V. Walter, M. Ghogho, and M. Saska, "Optical communication-based identification for multi-uav systems: theory and practice," *Autonomous Robots*, vol. 49, no. 3, p. 24, Sep 2025.

[15] T. Lakemann, D. B. Licea, V. Walter, T. Báča, and M. Saska, "Towards agile multi-robot systems in the real world: Fast onboard tracking of active blinking markers for relative localization," vol. 194, p. 105175.

[16] D. Scaramuzza, A. Martinelli, and R. Siegwart, "A Flexible Technique for Accurate Omnidirectional Camera Calibration and Structure from Motion," in *Fourth IEEE International Conference on Computer Vision Systems (ICVS'06)*, 2006-01, pp. 45–45.

[17] J. Horyna, V. Krátký, V. Pritzl, T. Báča, E. Ferrante, and M. Saska, "Fast Swarming of UAVs in GNSS-Denied Feature-Poor Environments Without Explicit Communication," *IEEE Robot. Autom. Lett.*, vol. 9, no. 6, pp. 5284–5291, Jun. 2024.